Measurement of Interface-Induced Optical Anisotropies of a Semiconductor Heterostructure: ZnSe/GaAs(100)

T. Yasuda,[1,2] K. Kimura,[1,3] S. Miwa,[1,3] L. H. Kuo,[1,3] C. G. Jin,[1,4] K. Tanaka,[1,2,4] and T. Yao[1,2,5]

[1]*Joint Research Center for Atom Technology (JRCAT), Tsukuba 305, Japan*
[2]*National Institute for Advanced Interdisciplinary Research, Tsukuba 305, Japan*
[3]*Angstrom Technology Partnership, Tsukuba 305, Japan*
[4]*University of Tsukuba, Tsukuba 305, Japan*
[5]*Institute for Materials Research, Tohoku University, Sendai 980, Japan*
(Received 26 October 1995)

We have developed a simple procedure that enables *in situ* simultaneous measurement of the surface and interface anisotropies in semiconductor heterostructures. Optical anisotropies in ZnSe/GaAs(100) heterostructures grown by molecular beam epitaxy were measured *in situ* by reflectance difference spectroscopy (RDS). We show that a Se treatment of the clean GaAs surface forms an optically anisotropic subsurface layer that remains intact even after ZnSe overgrowth, while a Zn treatment results in a quite different interface RD response. The RD spectra of the Se- and Zn-terminated ZnSe surfaces are briefly discussed. [S0031-9007(96)00536-4]

PACS numbers: 68.35.–p, 68.55.–a, 78.66.–w, 81.65.–b

Reflectance-difference, or reflectance-anisotropy, spectroscopy (RDS or RAS) has been emerging as a powerful tool to characterize solid surfaces in various environments [1,2]. For a materials system that is optically isotropic in the bulk, the observed anisotropy is due to the structural anisotropy at the surface and/or the buried interface. To date RDS has been used mainly to probe the surfaces of group III-V [3–5] and group IV [6–8] semiconductors. Application of the RD technique to interface studies has been limited to a few cases where the surface contribution was negligible [8,9]. In general, an RD signal from a heterostructure can contain both surface and interface contributions if the overlayer is optically transparent. In order to utilize fully RDS's potential capability as an interface probe, we need to establish a procedure to separate the two contributions.

This paper discusses surface- and interface-induced anisotropies of ZnSe/GaAs(100) heterostructures prepared by molecular beam epitaxy (MBE). The RD spectra at various ZnSe thicknesses and under different surface terminations are shown first. We then demonstrate a procedure to separate interface and surface contributions in these spectra. We will discuss the interface-formation process with an emphasis on the effect of pregrowth Se and Zn treatments on the GaAs substrate.

We emphasize that the analytic techniques presented are, in essence, also applicable to heterostructures other than ZnSe/GaAs. The ZnSe/GaAs structure is a good case for us to test the RDS's capabilities as an interface probe: Due to its heterovalent nature (II-VI on III-V), re-arrangements and/or reconstructions possibly take place at this interface to satisfy the electron-counting requirements [10,11], which is to be reflected in the optical anisotropy spectrum. While theory predicts diversity and complexity of the ZnSe/GaAs interface structures [11], experiments have provided only limited information about them [12–14]. The ZnSe/GaAs interface is of technological interest as well, because its integrity has a great impact on the performances of ZnSe-based light-emitting devices [15].

In RDS, one measures the difference between the normal-incidence reflectances for two orthogonal polarization directions in the surface plane. The results are commonly reported in terms of $\Delta\tilde{r}/\tilde{r} = \Delta r/r + i\Delta\theta$, where $\tilde{r} = r\exp(i\theta)$ is the complex reflectance. In this study $\Delta\tilde{r}$ is defined as $\Delta\tilde{r} = \tilde{r}_{\overline{1}10} - \tilde{r}_{110}$, were the subscript denotes the incident polarization vector. We will show only the $\Delta r/r$ spectra in this paper. Our RDS apparatus is similar to the one reported by Aspnes *et al.* [16].

The heteroepitaxial growth was carried out in a dual-chamber MBE system. First, an undoped GaAs buffer layer was deposited on a GaAs(100) wafer. The sample was then transferred *in vacuo* to another MBE chamber for the ZnSe growth, where RDS and reflection high-energy electron diffraction (RHEED) measurements were carried out. Prior to growth the GaAs surface was exposed to the Se beam for 10 s. The sample temperature was 533 K, and the beam-equivalent pressures of Se and Zn were 5.5×10^{-5} and 8.9×10^{-5} Pa, respectively. The growth rate of ZnSe was 0.061 nm/s under these conditions.

Figure 1 shows the RD spectra taken at different ZnSe thicknesses. The growth was interrupted at the thicknesses noted in the figure legend, and in each case the spectra were taken first under the Se beam [Fig. 1(a)] and then under the Zn beam [Fig. 1(b)]. From our RHEED measurements, the surface reconstructions under the Se and the Zn beams were, respectively, 2×1 and $c(2 \times 2)$, as commonly observed for MBE-grown ZnSe [17].

Comparing the spectra in Figs. 1(a) and 1(b) at the same thicknesses, we find that the RD response below 3.5 eV
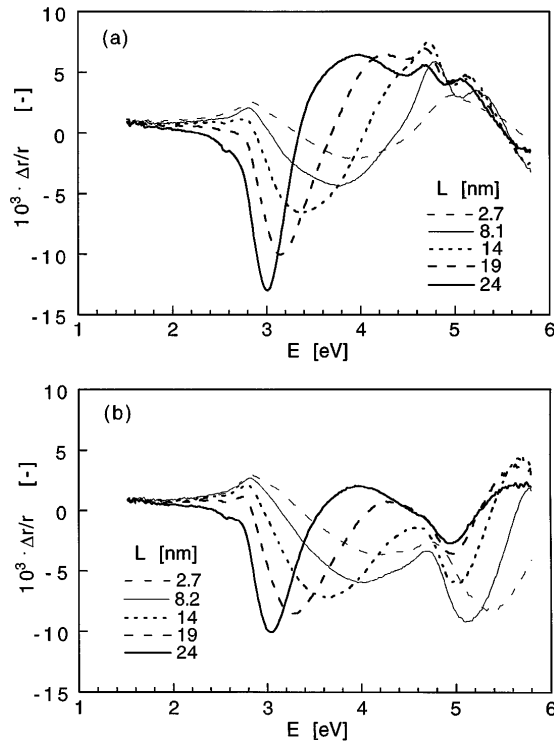
FIG. 1.   RD spectra of the ZnSe/GaAs heterostructure measured at different ZnSe thicknesses as indicated in the legend. The initial GaAs surface was treated with Se. (a) RD under the Se beam; (b) RD under the Zn beam.

is essentially unchanged by switching the surface termination. This observation indicates that the interface contribution dominates in this energy range. The apparent spectral evolution with ZnSe thickness is due to interference between the beams reflected at the ZnSe surface and at the ZnSe/GaAs interface. The mathematical procedure described below was used to remove the interference artifacts, and at the same time to separate the surface and interface contributions. It should be emphasized that while the band gap of ZnSe is 2.6 eV at the growth temperature the ZnSe layers studied in this experiment were thin enough to transmit light of up to 5 eV, thus permitting RDS investigation of the interface over a wide energy range.

In the conventional three-phase model which consists of a substrate (in the present case, GaAs), an overlayer (ZnSe), and an ambient (vacuum), $\tilde{r}$ is given as [18]

$$\tilde{r} = (Z\tilde{r}_{so} + \tilde{r}_{oa})/(1 + Z\tilde{r}_{so}\tilde{r}_{oa}), \qquad (1)$$

where $Z = \exp(4\pi i\tilde{n}_o L/\lambda)$, $\tilde{n}_o$ is the complex refractive index of the overlayer, L is the overlayer thickness, λ is the wavelength of light, $\tilde{r}_{oa}$ and $\tilde{r}_{so}$ are the complex reflectances at the overlayer-ambient and substrate-overlayer boundaries, respectively. In this equation, there are three variables that can be anisotropic: $\tilde{r}_{oa}$, $\tilde{r}_{so}$, and $\tilde{n}_o$. Mathematically, one can write a linear expression of a total derivative, $d\tilde{r}$, using the partial differentials of $\tilde{r}$ with respect to these three variables. By performing the partial-differential calculations, we obtain the following

expression:

$$\frac{\Delta\tilde{r}}{\tilde{r}} = A^{-1}\left(\frac{\Delta\tilde{r}_{oa}}{\tilde{r}_{oa}}B + \frac{\Delta\tilde{r}_{so}}{\tilde{r}_{so}}C + \Delta\tilde{n}_o C\frac{4\pi iL}{\lambda}\right), \quad (2)$$

with

$$A = (1 + Z\tilde{r}_{so}\tilde{r}_{oa})(Z\tilde{r}_{so} + \tilde{r}_{oa}), \qquad (3a)$$

$$B = \tilde{r}_{oa}(1 - Z\tilde{r}_{so})(1 + Z\tilde{r}_{so}), \qquad (3b)$$

$$C = Z\tilde{r}_{so}(1 - \tilde{r}_{oa})(1 + \tilde{r}_{oa}). \qquad (3c)$$

In the following text, $\Delta\tilde{r}_{oa}/\tilde{r}_{oa}$ and $\Delta\tilde{r}_{so}/\tilde{r}_{so}$ are called the surface and the interface anisotropies, respectively. In a physical sense, $\tilde{r}_{oa}$, $\tilde{r}_{so}$, and $\tilde{n}_o$ are not independent variables, all being a function of the overlayer dielectric response. Nevertheless, Eq. (2) is useful for us to identify which processes give rise to the observed anisotropy: the reflection at the surface or at the interface, or the propagation through the overlayer.

In the following analyses we neglect the $\Delta\tilde{n}_o$ term in Eq. (2). This approximation is adequate for the present case because L is much smaller than both λ and the critical thickness for plastic relaxation in ZnSe/GaAs [19]. The two quantities of interest, $\Delta\tilde{r}_{oa}/\tilde{r}_{oa}$ and $\Delta\tilde{r}_{so}/\tilde{r}_{so}$, can then be determined using two RD measurements at different thicknesses, L_1 and L_2.

We emphasize that this procedure involves no parameter fitting. Thus it enables us to monitor the surface and the interface simultaneously in real time. We note that one may better simulate the observed spectra using an optical model with more constituent layers, such as a five-phase model [i.e., ambient/(surface layer)/overlayer/(interface layer)/substrate]. The primary advantage of the Eq. (2) approach over such elaborated models consists in its simplicity. As we demonstrate below, Eq. (2) is useful in eliminating the interference artifact without introducing any fitting parameter, even when there exist bulk anisotropies in the substrate and the overlayer.

The interface and surface contributions separated using the above procedure are displayed in Figs. 2 and 3, respectively. In these figures, each spectrum was generated from the corresponding two source spectra in Fig. 1, as labeled in the legend. The line shapes are essentially independent of epilayer thickness, which confirms that the interference artifacts have been eliminated. In performing the calculation, we used the dielectric functions of GaAs at 500 K [20] and of ZnSe at 473 K [21]. Because the 473 K ZnSe data terminate at 5.1 eV, the calculated spectra also terminate at the same energy. For the (19 nm, 24 nm) spectra in both figures, the interface spectrum terminates at 4.3 eV and the surface spectrum continues up to 5.8 eV. The reason for this exception is that the 19 and 24 nm spectra in Fig. 1 have a negligible interfacial contribution above 4.3 eV due to strong absorption in the ZnSe epilayer.

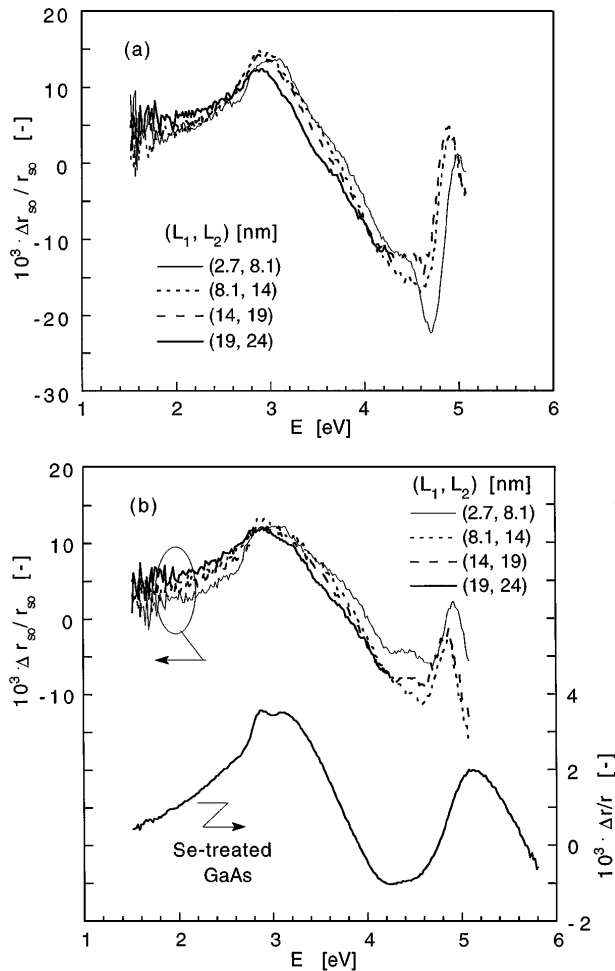First we discuss the interface RD spectra. Figure 2(a) and 2(b) are the interface RD spectra with Se and

FIG. 2. The interface contribution to the RD spectra in Fig. 1. Each spectrum was obtained from the two corresponding spectra in Fig. 1, as indicated in the legend. (a) Under the Se beam; (b) under the Zn beam. Also plotted in (b) is the RD spectrum of the Se-treated GaAs surface.

FIG. 3. As Fig. 2, but for the surface contribution. (a) Under the Se beam; (b) under the Zn beam. Also plotted in (a) is the energy-scaled Imε spectrum of ZnSe at room temperature (from Ref. [25]).

Zn surface terminations, respectively. The spectral line shapes below 4 eV are essentially the same for the two different ZnSe-surface terminations, which are consistent with their interfacial origin. The distinct features around 5 eV in both figures are presumably due to the linear electro-optic effect (LEOE), as discussed later in the text.

In Fig. 2(b), we also show the RD spectrum for the Se-terminated GaAs surface, which was the starting surface for the experiment in Fig. 1. A close resemblance in the spectra below 3.5 eV is apparent for the Se-terminated GaAs surface and those spectra obtained from ZnSe/GaAs interfaces. The RD intensity is, however, quite different. To make the comparison more quantitative, we have converted the interface and surface RD spectra in Fig. 2 into anisotropy spectra of the dielectric response, $\Delta(\varepsilon d)$. In performing this conversion we used an RD expression for the surface anisotropy, which assumes a three-phase model [22]. In brief, the model assumes an optically anisotropic thin layer at the boundary between
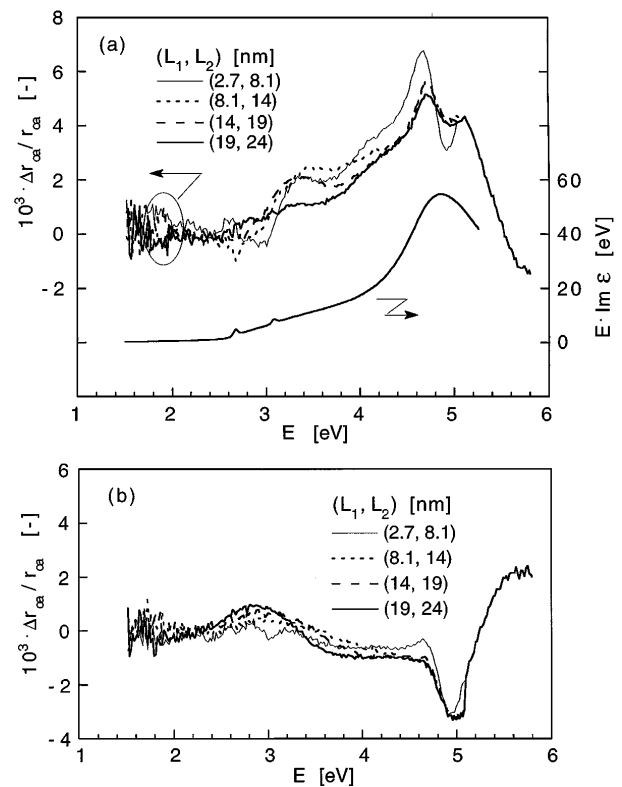
two isotropic media, whose thickness, d, satisfies $d \ll \lambda$. $\Delta(\varepsilon d)$ of this thin layer is defined, in the present case, as $\Delta(\varepsilon d) = (\varepsilon_{\bar{1}10} - \varepsilon_{110})d$, where $\varepsilon_{\bar{1}10}$ and ε_{110} are the complex dielectric functions for polarization vectors parallel to the $[\bar{1}10]$ and $[110]$ directions, respectively.

In Fig. 4, the thin solid curve is the imaginary part of $\Delta(\varepsilon d)$ for the ZnSe/GaAs interface, while the dotted curve is that for the Se-terminated GaAs. Below 3.5 eV the two spectra agree in both line shape and intensity. This agreement strongly suggests that the Se treatment of the GaAs surface formed an anisotropic subsurface layer which was the origin of the RD signal below 3.5 eV, and that this subsurface layer maintained its structure during ZnSe epilayer growth.

While further studies are needed to determine the detailed structure of the anisotropic layer, one comment can be made at the present stage. Li *et al.* reported that a Ga_2Se_3 interfacial layer was formed in the case of a ZnSe/GaAs sample processed at a relatively high temperature [12]. Li and Pashley proposed, based on the electron counting model, that the Se-treated GaAs surface has a subsurface structure analogous to Ga_2Se_3 [23]. Although Ga-Se bonds are presumably involved in the anisotropic layer of our sample, the $\Delta(\varepsilon d)$ spectra in Fig. 4 do not exhibit any features at the critical-point energies of the known Ga-Se compounds [24]. For example, one would

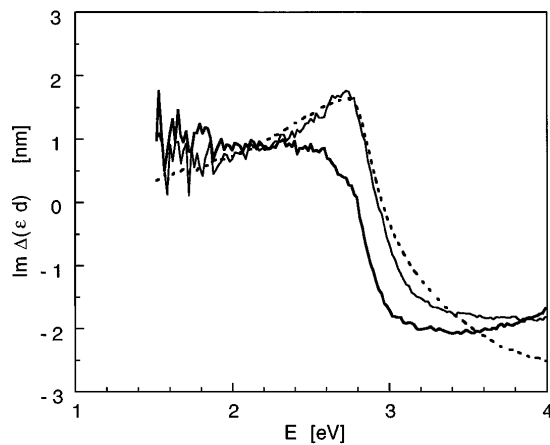FIG. 4. Imaginary part of $\Delta(\varepsilon d)$. Dotted curve: Se-treated GaAs surface; thin solid curve: ZnSe/GaAs interface formed on Se-treated GaAs; thick solid curve: ZnSe/GaAs interface formed on Zn-treated GaAs. For the interface, the (8.1 nm, 14 nm) spectra under the Zn beam are shown because they are representative of the spectra at different ZnSe thicknesses.

expect spectral features at the E_0 and E_1 transitions of zino-blende Ga_2Se_3 which are at 2.1 and 3.9 eV, respectively.

In order to investigate the effects of the predeposition treatment, a GaAs substrate surface was prepared by exposure to the Zn beam, instead of the Se beam. The interface RD spectrum for the Zn-treated sample was converted into $\Delta(\varepsilon d)$, and the result is displayed in Fig. 4. Compared to the Se treatment, the Zn-treated sample shows a much reduced intensity at 2.8 eV, indicating that the formation of the subsurface layer was suppressed. This demonstrates that the ZnSe/GaAs interfacial structure can, in fact, be controlled by different predeposition treatment.

Now we discuss the surface contributions shown in Fig. 3. We have found that the surface RD spectra under the Se beam resembles the imaginary part of the ZnSe dielectric-function spectrum, $Im\varepsilon(E)$. In Fig. 3(a), an energy-scaled spectrum, $E\,Im\varepsilon(E)$, at room temperature is shown for comparison [25]. Following Aspnes [22], we interpret this line shape as the result of anisotropic many-body screening at the ZnSe surface. The surface under the Zn beam shows a relatively small anisotropy below 4.5 eV [see Fig. 3(b)], which is consistent with the absence of anisotropic dimer structures at the $c(2 \times 2)$ ZnSe surface [26].

Finally, we address the spectral signatures due to LEOE. As for the GaAs homostructure, the LEOE-originating RD signals are reported to appear at the E_1 and $E_1 + \Delta_1$ critical points when it is doped to develop significant band bending at the surface [27,28]. In a heterostructure where a built-in field commonly exists, the RD spectra are likely to be decorated by LEOE signatures. If the overlayer is thin, as is the case in the present study, the charges at the surface and the interface can affect the field profile across the overlayer and thereby

the magnitude of the LEOE features. In all the spectra in Figs. 2 and 3, we indeed notice distinct features around 5 eV, which we ascribe to the LEOE associated with the E_1 and $E_1 + \Delta_1$ critical points of ZnSe. A close examination of these features has revealed that the sign of the built-in field with respect to the growth direction was positive in the entire ZnSe layer, regardless of the surface termination.

In summary, we have demonstrated the *in situ* and simultaneous characterization of the surface and interface by RDS. Extensive efforts are under way to identify experimentally the whole range of the possible ZnSe/GaAs interface structures, and to correlate them to the defect formation.

[1] D. E. Aspnes, Thin Solid Films **233**, 1 (1993).
[2] B. Drevvillon and V. Yakovlev, in *Physics of Thin Films,* edited by M. H. Francombe and J. L. Vossen (Academic Press, San Diego, 1994), Vol. 19, p. 2.
[3] I. Kamiya *et al.,* Phys. Rev. B **46**, 15 894 (1992).
[4] F. Reinhardt *et al.,* J. Vac. Sci. Technol. B **11**, 1427 (1993).
[5] J. Jonsson *et al.,* J. Appl. Phys. **70**, 1737 (1991).
[6] A. R. Turner *et al.,* Phys. Rev. Lett. **74**, 3213 (1995).
[7] T. Yasuda *et al.,* Phys. Rev. Lett. **74**, 3431 (1995).
[8] T. Yasuda *et al.,* J. Vac. Sci. Technol. A **12**, 1152 (1994).
[9] Z. Yang *et al.,* Appl. Phys. Lett. **66**, 2235 (1995).
[10] M. D. Pashley, Phys. Rev. B **40**, 10 481 (1989).
[11] K. Oda and T. Nakayama, Jpn. J. Appl. Phys. **31**, 2359 (1992).
[12] D. Li *et al.,* Appl. Phys. Lett. **57**, 449 (1990).
[13] M. S. Yeganeh *et al.,* Phys. Rev. B **49**, 11 196 (1994).
[14] R. Nicolini *et al.,* Phys. Rev. Lett. **72**, 294 (1994).
[15] L. H. Kuo *et al.,* J. Vac. Sci. Technol. B **13**, 1694 (1995).
[16] D. E. Aspnes *et al.,* J. Vac. Sci. Technol. A **6**, 1327 (1988).
[17] T. Yao and T. Takeda, Appl. Phys. Lett. **48**, 160 (1986).
[18] D. E. Aspnes, in *Optical Properties of Solids: New Developments,* edited by B. O. Seraphin (North-Holland, Amsterdam, 1976), p. 799.
[19] J. Petruzzello *et al.,* J. Appl. Phys. **63**, 2299 (1988).
[20] P. Lautenschlager *et al.,* Phys. Rev. B **35**, 9174 (1987).
[21] R. W. Collins and J. Lee (private communication).
[22] D. E. Aspnes, J. Vac. Sci. Technol. B **3**, 1498 (1985).
[23] D. Li and M. D. Pashley, J. Vac. Sci. Technol. B **12**, 2547 (1994).
[24] G. Guizzetti *et al.,* J. Phys. Soc. Jpn. **49**, 93 (1980).
[25] S. Adachi and T. Taguchi, Phys. Rev. B **43**, 9569 (1991).
[26] A. Garcia and J. E. Northrup, Appl. Phys. Lett. **65**, 708 (1994).
[27] V. L. Berkovits and D. Paget, Thin Solid Films **233**, 9 (1993).
[28] H. Tanaka *et al.,* Appl. Phys. Lett. **59**, 3443 (1991).